The Isothermal Oxidation Behavior of a Ti_3Al-Nb-V-Mo Alloy

Ying Wu[*,1] and Gui Ming Song[2]

[1]*School of Materials Science and Engineering, Shanghai Institute of Technology, No. 120, Cao Bao Road, Shanghai, 200235, P.R. China*

[2]*Department of Materials Science and Engineering, Delft University of Technology, Mekelweg 2, 2628CD Delft, The Netherlands*

Abstract: The isothermal oxidation behavior of Ti-24Al-14Nb-3V-0.5Mo alloy in synthetic air from 700°C to 1000°C was studied. The main emphasis was focused on the effect of microstructure obtained by different processes of melting and hot rolling, i.e. large β and duplex of α_2+B2, on the oxidation resistance. Regardless of the microstructure, the overall oxidation process of the specimens exposed at 700°C was dominantly controlled by the beneficial effect of Nb-addition due to the formation of a continuous α-Al_2O_3 layer in the scale. However, both specimens showed poor oxidation resistance above 900°C, especially for the as-rolled specimen, because of higher volume fraction of the α_2-phase. The spallation occurred in both specimens at 1000°C, which was probably relative to the formation of Ti_2AlN between the thick scale and the substrate except for the TiO_2 and α-Al_2O_3.

Keywords: Ti_3Al-Nb alloy, rolling, melting, microstructure, oxidation.

1. INTRODUCTION

Titanium aluminides such as α_2-Ti_3Al and γ-TiAl are potential high-temperature structural materials for aerospace applications due to their relatively low density, good elevated temperature strength and excellent creep behavior at high temperatures [1]. The β-phase (bcc) stabilizing elements such as Nb, V and Mo are usually added in Ti_3Al-based alloys to ameliorate the ductility, and a duplex microstructure containing α_2 and β-phase forms at temperatures below the β-transus temperature, T_β. A pseudo-binary Ti_3Al system with Nb addition is referred in literature [2]. Nb is known to be the most effective element for improving the mechanical properties especially for the room temperature ductility by activating non-basal slip, and to induce significant improvement of oxidation resistance of Ti_3Al-based alloys [3-5]. Actual applications in the aerospace industry and laminated compositions require the alloys to be considered in a variety of high-temperature environments. Most work on the oxidation behavior of Ti_3Al-based alloys concerns the effect of the alloying elements Nb and Si on improvement of oxidation resistance by surface modification [6-12], however, the effect of microstructure on the oxidation behavior of 14at.%Nb-containing Ti_3Al-based alloy is still lacking. The formation mechanism and microstructural development of the O-phase as well as the tensile deformation and fracture behavior of Ti_3Al-Nb alloy have been previously studied by Wu *et al*. [13-16]. The purpose of the present study, therefore, is to evaluate the isothermal oxidation behavior of Nb, V and Mo-containing Ti_3Al-based alloy by focusing on the effect of microstructure on the oxidation resistance.

*Address correspondence to this author at the School of Materials Science and Engineering, Shanghai Institute of Technology, No. 120, Cao Bao Road, Shanghai, 200235, P.R. China; Tel/Fax: 86-21-64942815; E-mail: yingwu2000@hotmail.com

2. EXPERIMENTAL

A nominal chemical composition of the experimental materials used in the present studies is Ti-24Al-14Nb-3V-0.5Mo Alloy (at.%), which was obtained by triple melting in a vacuum consumable electrode arc melted furnace. The as-cast pancake was first forged at 1250-1280°C in the β region, and then forged in the α_2+β region to a billet followed by air cooling. The as-rolled specimen was obtained by hot-rolling to about 2mm thickness at an adequate temperature with a small amount of deformation at each pass. The as-melted specimen was used to compare the oxidation behavior.

The specimens of $6\times8\times2mm^3$ were prepared by electrodischarge machining for the oxidation test. Surface of the specimens was polished with 1000 grit SiC paper followed by ultrasonic cleaning for 15 min in a methanol solution. Isothermal oxidation tests of the specimens were conducted using a thermogravimetric analyzer (TG-DTA2000SA) to record continuous mass change as a function of time in synthetic air (21% O_2 and 79% N_2) with a flow of 200 ml/min from 700 to 1000°C up to 120h. The heating and cooling rates of the specimens were 50°C/min. The spalled oxides could be weighed together with the oxide scales.

Microstructural observation of the as-melted and as-rolled specimens was performed by optical microscopy. Morphologies on the surface and cross-sections of oxide scales were examined by scanning electron microscopy (SEM, JSM-6500). Distribution of elements in the oxide scales was analyzed by energy-dispersive X-ray spectrometry (EDS) and mapping in a SEM. The identification of crystalline phases of the oxide scales was made by X-ray diffractometry (XRD) using Cu (K_α) as a target.

1876-5033/10 2010 Bentham Open

3. RESULTS

3.1. Microstructure Priors to the Oxidation

Fig. (**1**) shows optical micrographs of the as-melted and as-rolled Ti_3Al-Nb-V-Mo alloy. As shown in Fig. (**1a**), the as-melted specimen showed a very simple microstructure consisting of β phase with a coarse grain. In the as-rolled specimen, see Fig. (**1b**), a duplex microstructure consisted of equiaxed primary α_2-phase and continuous matrix of B2-phase (ordered β), which evidenced by the results of the XRD, as shown in Fig. (**2**). TEM observation indicated that the microstructure in the as-rolled specimen consists of the primary equiaxed α_2-phase, a considerable amount of B2-phase matrix and fine O-phase formed within the primary α_2 grain [14-16]. Thus, the observed microstructure in the as-rolled specimen represented a typical recrystallized structure after thermo-mechanical treatments.

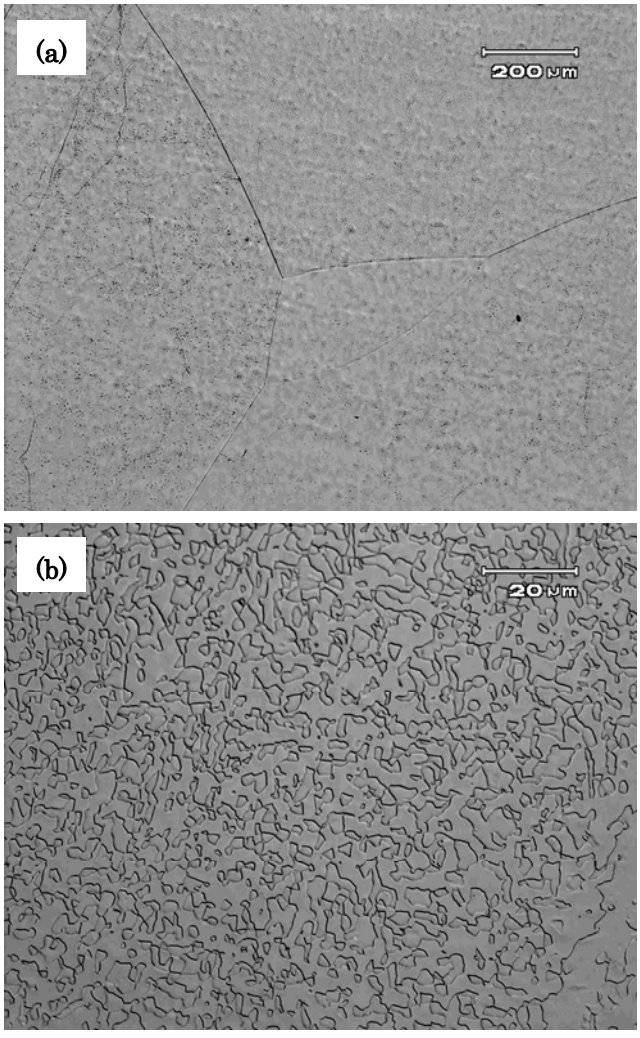

Fig. (1). Optical micrographs showing the microstructure of Ti-24Al-14Nb-3V-0.5Mo alloy produced by (**a**) melting and (**b**) hot rolling processing. The microstructures show single β phase and α_2+β two-phase corresponding to (**a**) and (**b**), respectively.

3.2. Isothermal Oxidation Kinetics

Fig. (**3**) shows isothermal oxidation behavior of the Ti_3Al-Nb-V-Mo alloy exposed in synthetic air at 700, 800, 900 and 1000°C up to 120h. All the mass gain curves obeyed a parabolic trend. For the mass gain curves of the specimens at 1000°C, two segments in the curves displayed a parabolic relationship. The values (K_p) of rate constant of 45.6 g^2m^{-4}/h (0-72h) and 73.6 g^2m^{-4}/h (72h-120h) for the as-melted specimen, and 74.4 g^2m^{-4}/h (0-87h) and 80.8 g^2m^{-4}/h (87-120h) for the as-rolleded specimen were determined, respectively, indicating a much higher oxidation rate in the latter. Regardless of the as-melted and as-rolled specimen, the mass gain increased with increasing the exposure temperatures from 700 to 1000°C, and the mass gain kept almost the same increase between 700 and 900°C, they were 5.3 and 6.7, 34.2 and 35.1, 44.8 and 45.4 for the as-melted and as-rolled specimen, respectively. However, the as-rolled specimen showed higher mass gain than the as-melted one at 1000°C, it was 104.4 and 99.0 g/m^2, respectively, indicating that the as-rolled specimen exposed above 900°C exhibits a faster growth of the oxide scale.

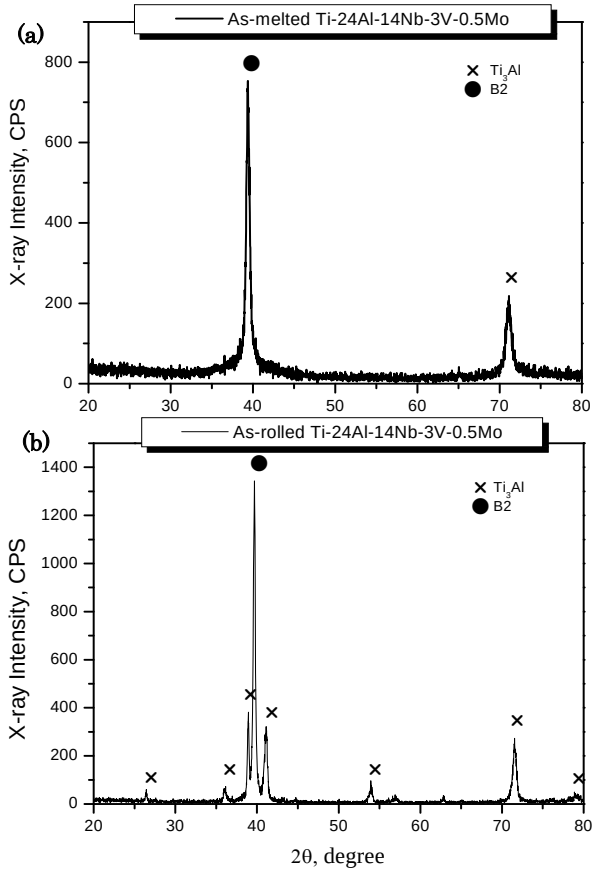

Fig. (2). XRD spectra of Ti-24Al-14Nb-3V-0.5Mo alloy prior to oxidation: (**a**) the as-melted and (**b**) as-rolled.

3.3. XRD Phase Analysis

The constitutes of the oxide scales depended on the exposure temperature. XRD spectra of the oxide scales of the Ti_3Al-Nb-V-Mo specimen isothermally exposed for 120h at 700 and 1000°C are shown in Fig. (**4a-d**), respectively. Regardless of the as-melted and as-rolled specimen, the major phases consisted of B2, α_2-Ti_3Al, TiO_2 (rutile) and

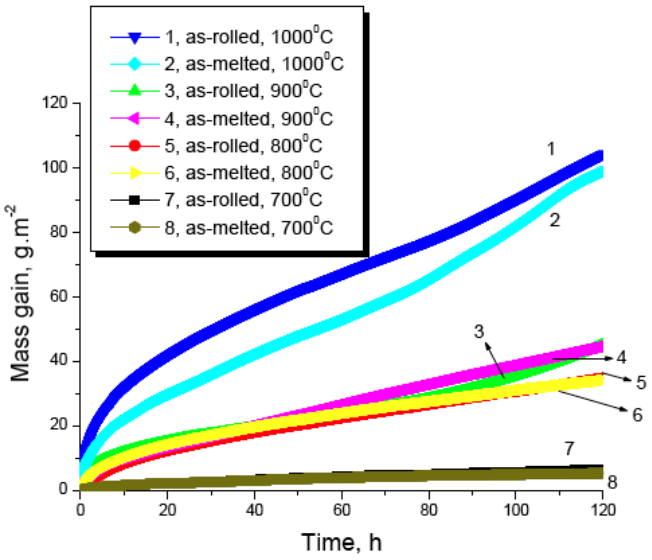

Fig. (3). Isothermal oxidation kinetics of the as-melted and as-rolled Ti-24Al-14Nb-3V-0.5Mo alloy in synthetic air at 700, 800, 900 and 1000°C.

α-Al_2O_3 for both specimens at 700°C, see Fig. (**4a**, **b**). The intensity of peaks from TiO_2 was the strongest among the four phases. The peaks from the substrate phases were also detected due to the thin scale. The oxides for the as-melted and as-rolled specimen had a similar case at 800 and 900°C, and the oxide scale consisted of TiO_2 and α-Al_2O_3. However, the oxide produces at 1000°C was different. The nitride of Ti_2AlN was detected in the scale for both as-melted and as-rolled specimen except for TiO_2 and α-Al_2O_3. In addition, some peaks of B2 and α_2-Ti_3Al from the underlying substrate were detected in both specimens due to the scale spallation under this temperature exposure.

3.4. Surface Morphology

Fig. (**5**) shows SEM micrographs of the surface morphology of the oxide scales of the alloy after 120h isothermal exposure at 700 and 1000°C. The size of oxides increases with increasing the exposure temperature. The oxide scale of both specimens exposed at 700°C exhibits a finer microstructure than that at 1000°C (Fig. **5a**, **b**), and the fine-grained microstructure of acicular oxides was uniformly covered on the surface of the specimens except for a small quantity of granular oxides. EDS analysis revealed that these

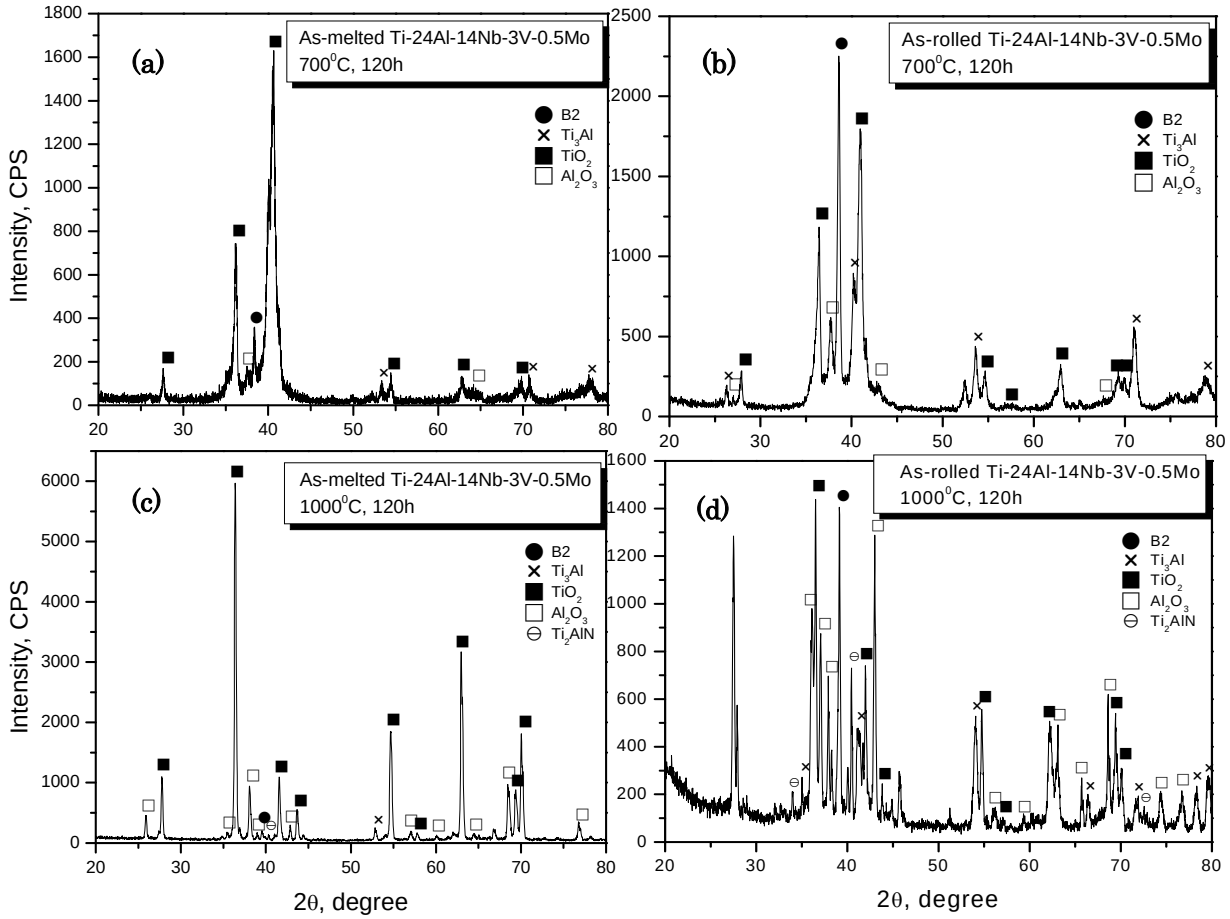

Fig. (4). XRD spectra of the oxide scale of the oxide scale after 120h isothermal oxidation at 700°C in (**a**) the as-melted and (**b**) the as-rolled Ti-24Al-14Nb-3V-0.5Mo alloy, and at 1000°C in (**c**) the as-melted and (**d**) the as-rolled alloy, respectively.

granular oxide particles were rich in oxygen and titanium. As for the acicular oxides, they were determined to be Al_2O_3 on the surface of both specimens. In the case of the as-melted and as-rolled specimen, surface morphology after isothermal exposure at 1000°C showed no significant difference from that of the specimens oxidized at 700°C except that there were larger oxide grains in the former (Fig. **5c**, **e**). The surface of both specimens was coved by the coarse granular oxides, which was rich in oxygen and titanium by EDS analysis. Especially to be noted that the spallation on the surface of both specimens occurred, see Fig. (**5d**, **f**).

3.5. Cross-Sectional Morphology

Fig. (**6a-d**) show typical SEM micrographs of a cross-section through a part of the scale formed on the alloy

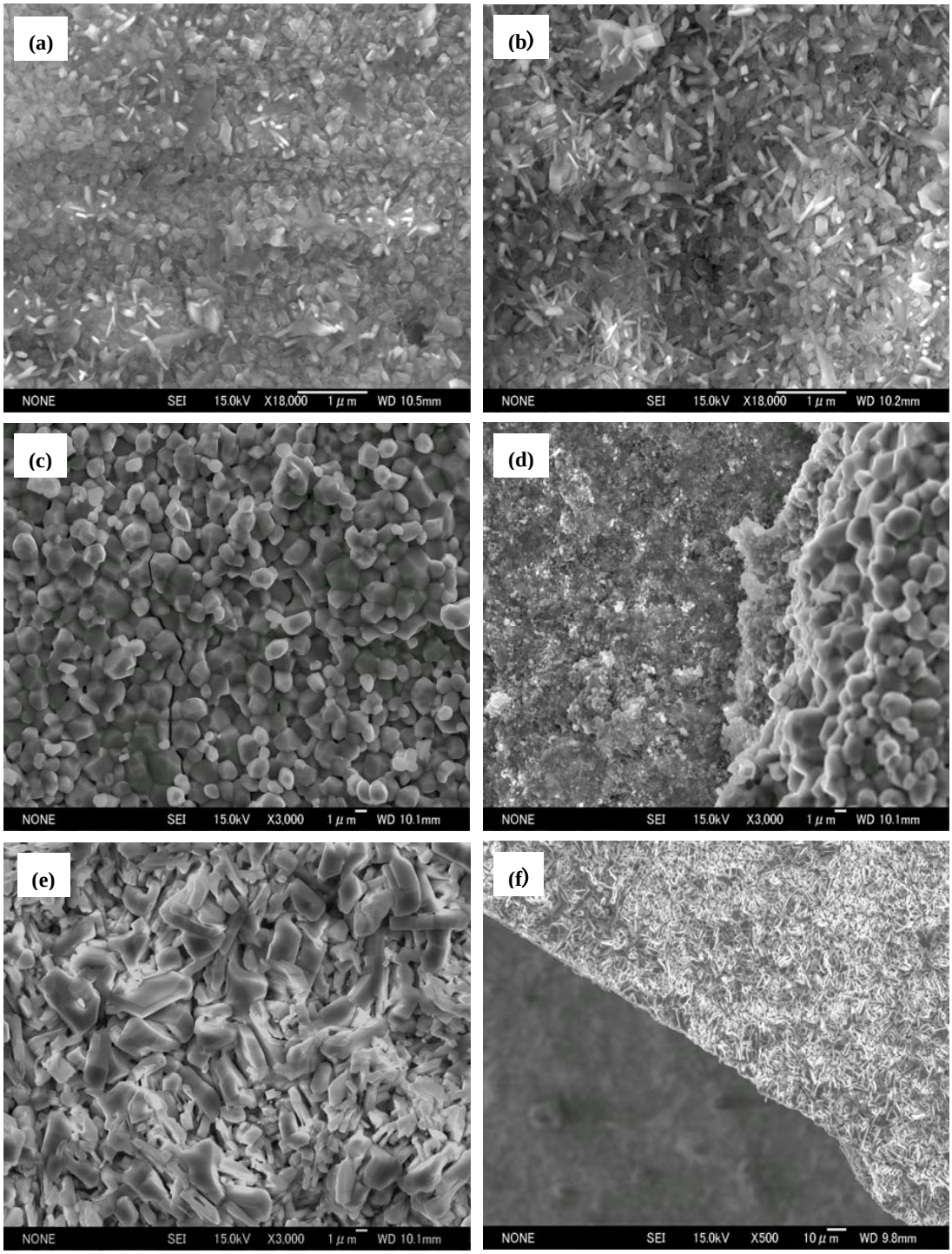

Fig. (5). SEM micrographs of the surface morphologies of the oxide scale after 120h isothermal oxidation at 700°C in (**a**) the as-melted and (**b**) the as-rolled Ti-24Al-14Nb-3V-0.5Mo alloy, and at 1000°C in (**c**) and (**d**) the as-melted, (**e**) and (**f**) the as-rolled alloy, respectively.

surface after 120h isothermal exposure at temperatures between 700 and 1000°C. The thickness of the oxide scale increased gradually as the exposure temperature increased. The thickness of the scale in the as-melted and as-rolled specimen oxidized at 700 and 1000°C was approximately 1, 1, 30 and 35μm, respectively. For both specimens exposed at 700°C in Fig. (**6a**, **b**), no microcracks were observed, indicating a good adhesion between the scale and substrate. With increasing the exposure temperature up to 1000°C, both scales showed a similar structure and morphology and thick scales formed on the surface of two specimens as shown in Fig. (**6c**, **d**).

Fig. (**7**) shows element distribution maps in cross section of the as-melted Ti-24Al-14Nb-3V-0.5Mo alloy isothermally oxidized for 120h by means of SEM-EDS. Scale structure of the specimen oxidized at 700°C was relatively simple, and in the order of mixed α-Al_2O_3+TiO_2 layer and a continuous α-Al_2O_3-rich layer from the inside layer. As shown on the Al map of Fig. (**7b**), the distribution of Al was homogeneous and continuous followed by a Al+Ti-mixed oxide scale.

However, only one type of oxide scale with simple composition was identified in the outer layer of the as-melted and as-rolled specimens exposed at 1000°C as shown in Figs. (**8a-f**). EDS analysis showed that the oxide scale near the substrate was composed of a large quantity of TiO_2 and a small quantity of α-Al_2O_3 mixture although there were a few of discontinuous α-Al_2O_3-rich regions on the Al map, see Fig. (**8b**).

4. DISCUSSION

Oxidation behavior of the Ti-24Al-14Nb-3V-0.5Mo alloy in the present study demonstrated that the microstructure, i.e., large β and duplex of α_2+B2, played a neglected effect below the exposure temperature of 900°C, in which the

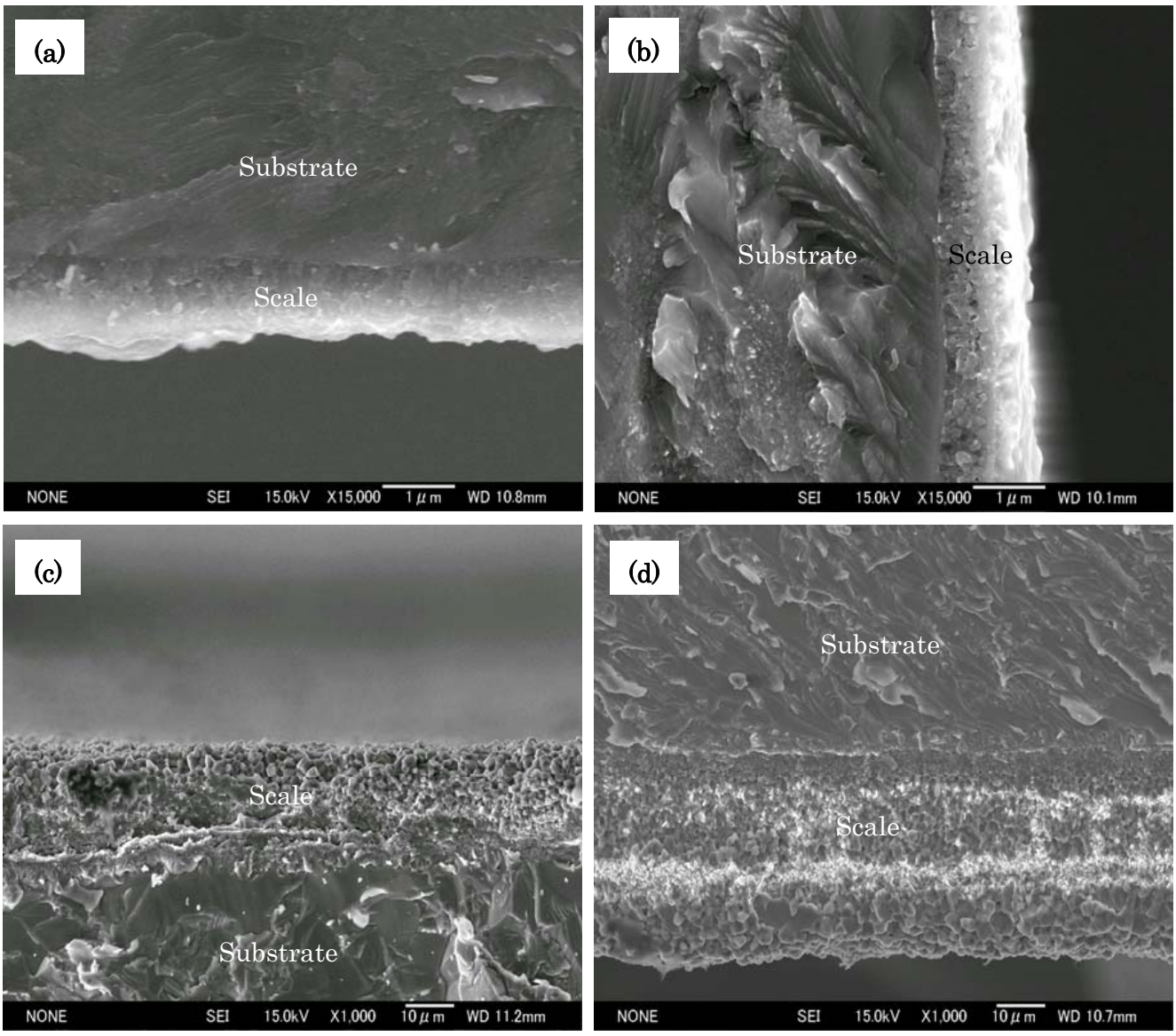

Fig. (6). SEM micrographs of the cross-sectional morphologies of the oxide scale after 120h isothermal oxidation at 700°C in (**a**) the as-melted and (**b**) the as-rolled Ti-24Al-14Nb-3V-0.5Mo alloy, and at 1000°C in (**c**) the as-melted and (**d**) the as-rolled alloy, respectively.

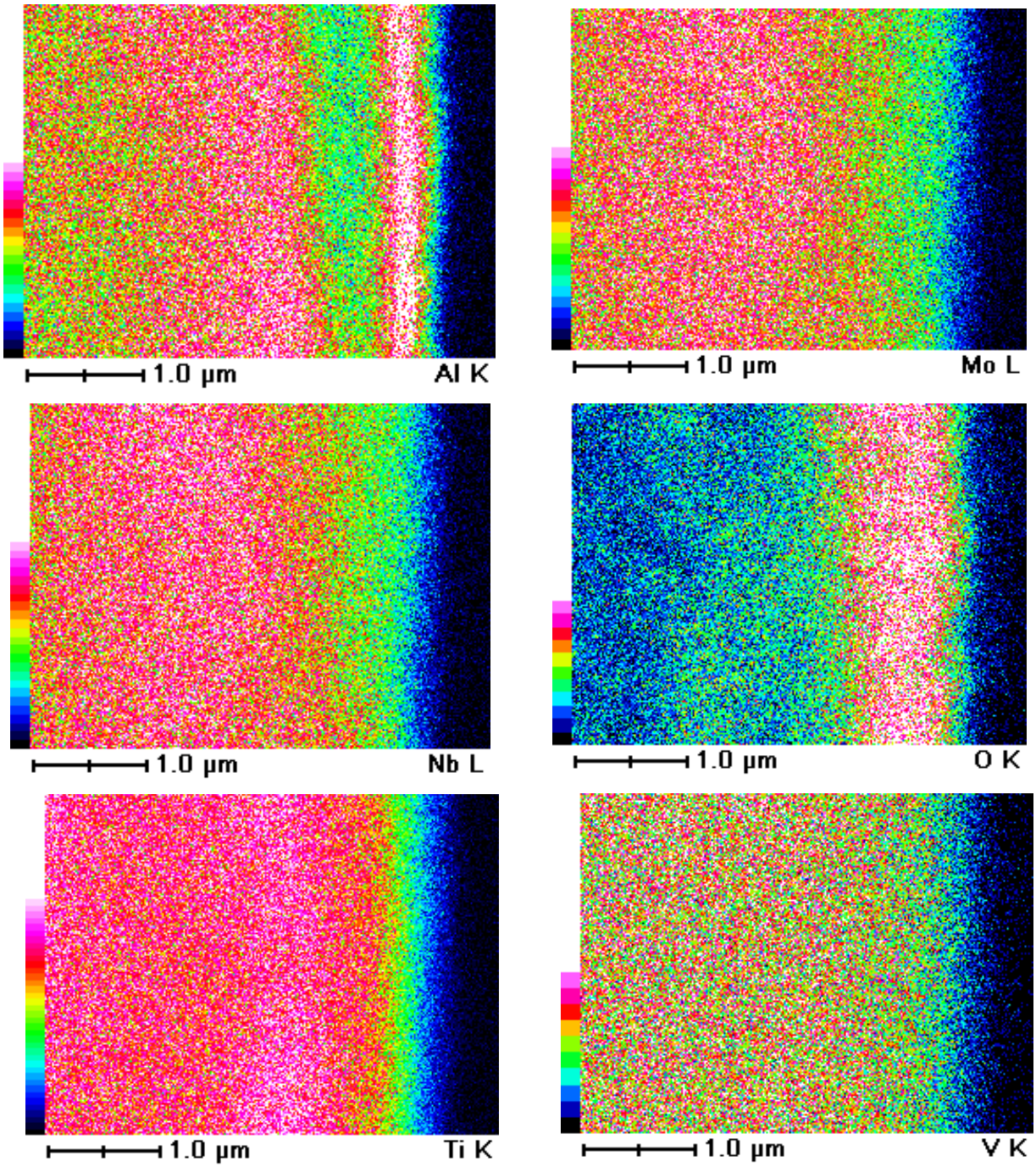

Fig. (7). Element distribution maps in cross section observed by means of SEM in the as-rolled Ti-24Al-14Nb-3V-0.5Mo alloy after isothermal oxidation at 700°C for 120h: (**a**) Ti, (**b**) Al, (**c**) Nb, (**d**) V, (**e**) Mo and (**f**) O.

effect of Nb was a main factor for controlling the oxidation rate during the exposure. In the as-rolled specimen, because the equiaxed α_2-phase and B2-phase are main, and their volume fraction is more than 90%, the effect of O-phase on the oxidation behaviour of Ti_3Al-Nb alloy, due to slight amount of O-phase within the α_2 grains, is usually omitted. The as-rolled specimen showed a faster oxidation rate above 900°C than the as-melted one. Thus, the effect of Nb depended on the exposure temperature. As shown in Fig. (**3**), both as-melted and as-rolled specimen containing 14at.%Nb showed better oxidation resistance at 700°C exposure than that at other temperatures, and small mass gains were obtained. The present results of mass gain curves differed from the results of Ti-23Al-10.3Nb-4.5V-0.9Cr alloy at 700-900°C as reported by Tomasi and Gialanella [17], in which the weight gain curves showed a parabolic trend up to 25h, due to the growth of a compact oxide scale on the surface, but at the time longer than 50h the mass gain-exposure time showed a linear relation. Similar mass gain curves and parabolic rate constant were obtained by Wallace *et al*. [18], they studied oxidation behavior of Ti-25Al-10Nb-3V-1Mo alloy at 650-1000°C in air, and found that the oxidation kinetics was complex and displayed up to two distinct stages of parabolic oxidation.

Regardless of the microstructure, the overall tendency of oxidation resistance of the Ti-24Al-14Nb-3V-0.5Mo alloy was poor when the exposure temperature increased above 900°C. XRD spectra showed that all the scales are composed of a mixture of TiO_2 and α-Al_2O_3 after isothermal oxidation for 120h. However, the quantity of α-Al_2O_3 in the oxide scale of both specimens oxidized at 700°C significantly increased (Fig. **4a**, **b**), and the surface morphology showed a fine and dense microstructure (Fig. **5a**, **b**) with the thinnest scale (Fig. **6a**, **b**). EDS analysis showed that the surface oxides consist of TiO_2-rich granular and α-Al_2O_3-rich acicular oxides in both the specimens, however, the specimen oxidized at 700°C was mainly covered by α-Al_2O_3-rich acicular oxides. A continuous α-Al_2O_3-rich layer formed to prevent the diffusion of oxygen as shown in the Al map of Fig. (**7b**). With increasing the exposure temperature up to 1000°C, the oxide grains grew rapidly. As shown in Fig. (**5c**, **d**), the surface oxides in the specimens consisted mostly of TiO_2 crystals since the growth rate of TiO_2 is higher than that of α-Al_2O_3. Ti was enriched in the overall oxide layer except for some discontinuous Al-rich regions as shown in the elements distribution maps in Fig. (**8b**). Nitrides of Ti_2AlN formed in the scale under higher oxidation temperature of 1000°C. Lang and Schütze [19] found that TiN and Ti_2AlN formed at the interface beneath a mixture of Al_2O_3+TiO_2. The formation of Ti_2AlN was believed to be relative to the adhesion of the scale and the substrate.

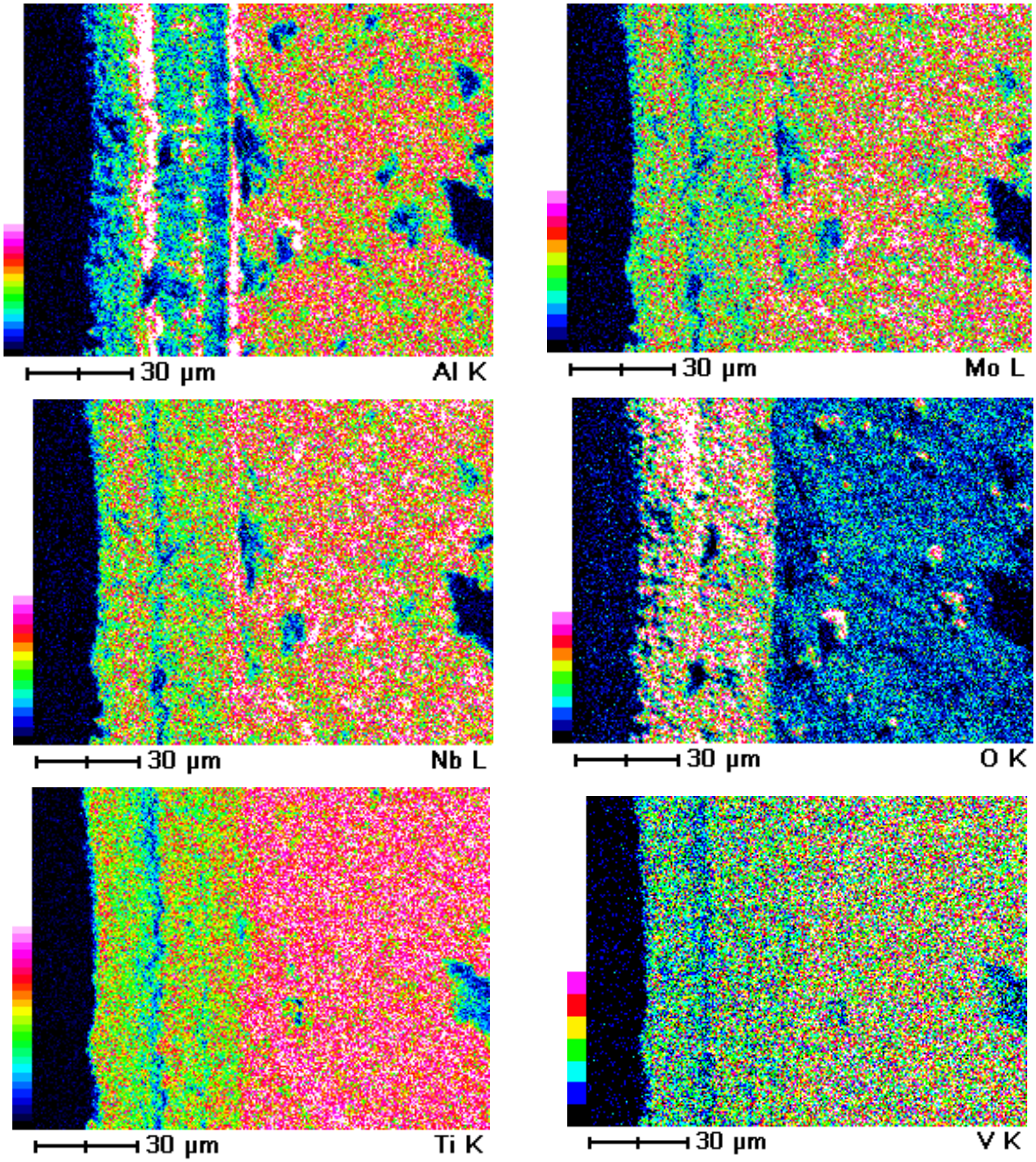

Fig. (8). Element distribution maps in cross section observed by means of SEM in the as-melted Ti-24Al-14Nb-3V-0.5Mo alloy after isothermal oxidation at 1000°C for 120h: (**a**) Ti, (**b**) Al, (**c**) Nb, (**d**) V, (**e**) Mo and (**f**) O.

The development mechanism of the scale formed on the Ti_3Al-Nb alloy supports the issue on promoting the formation of a continuous protective α-Al_2O_3 layer by addition of Nb, but it occurs at limited exposure temperatures. The beneficial effect of the alloying element Nb was obtained for the specimen exposed at 700°C and the oxidation resistance was improved due to the development of a continuous α-Al_2O_3 scale in the outer layer. Various mechanisms on the effect of Nb on the oxidation behavior of Ti-Al based alloys have been proposed. Wu *et al*. [7] studied effect of Nb (0-20at.%) on the oxidation behavior of Ti-25Al alloy at 800 and 900°C. They suggested that improvement of the oxidation resistance in the alloys by Nb-addition was attributable to the formation of a compact scale, which was favored not only by doping effect but also by the TiN layer which obstructed the outward Al diffusion into the scale to form porous intermixed TiO_2 and α-Al_2O_3. In the present study, the beneficial effect of Nb was to develop a continuous α-Al_2O_3 scale in the alloy containing 14at.%Nb under 700°C isothermal oxidation. No TiN was detected in the scale. Previous results in [20] showed that the Nb content was much higher than V content in the outermost TiO_2 oxide scales in the specimen oxidized at 900°C. According to the valence-control rule [21], defect concentrations in TiO_2 lattice are reduced depending on the solution of Nb in TiO_2 to form a compact scale on the substrate and hence improve the oxidation resistance. Therefore, the doping effect of Nb was active to improve oxidation resistance of the alloy oxidized at 700°C.

Concerning the effect of V and Mo on the oxidation behavior of the Ti_3Al-based alloy, the detailed studies are described elsewhere [20]. It was reported that V has a largely detrimental effect on oxidation, namely its oxides may dissolve the protective layers and enhance ionic conductivity through the scale [22]. These phenomena may accelerate the oxidation. Mo is generally regarded as a beneficial element for oxidation resistance of Ti-Al based alloys because of its doping effect in TiO_2.

The present study demonstrated that the as-rolled specimen showed a higher oxidation rate of the scale than the as-melted one, this was probably due to the large amount of the α_2-phase in the former. It was reported by Gil *et al*. [23] that at high-temperature exposure the γ-TiAl phase acts to form α-Al_2O_3, whereas the α_2-Ti_3Al phase induces formation of TiO_2. This difference in oxidation behavior is caused by the large difference in Ti and Al content s between the two phases. Because Al content in the α_2-phase is significantly low, the α_2-phase rapidly forms a TiO_2 scale when exposed at high temperatures. The large volume change induced by the formation of TiO_2 during the oxidation of inner α_2-Ti_3Al lamellae is believed to break up the outer α-Al_2O_3-rich film. This film impairment would easily occur in the as-rolled alloy due to the greater distortion by oxidation of coarser α_2-Ti_3Al phase. The inward diffusion of oxygen through the oxide scales could form a α-Al_2O_3-rich oxide, resulting in the development of a α-Al_2O_3+TiO_2 mixed layer. Therefore, the high volume fraction of α_2-Ti_3Al phase in the rolled alloy was mainly responsible for its poor oxidation resistance due to the fast growth of TiO_2.

5. CONCLUSIONS

Morphological characteristics of the oxide scales formed in the as-melted and as-rolled Ti_3Al-Nb-V-Mo alloy were studied under isothermal exposure at 700-1000°C for 120h, from the effect of microstructure on the oxidation resistance the following conclusions were drawn:

1. The microstructure of large β and duplex of α_2+B2 was obtained for the as-melted and as-rolled alloy, respectively. The microstructure played a neglected effect below 900°C exposure. The overall oxidation process of both specimens exposed at 700°C was dominantly controlled by the beneficial effect of Nb-addition to promote development of a continuous α-Al_2O_3 layer in the scale due to the doping effect. However, the oxidation resistance of specimens oxidized above 900°C was poor because of fast diffusion of oxygen.

2. Both specimens showed poor oxidation resistance above 900°C, especially for the as-rolled specimen, because of higher volume fraction of the α_2-phase. The spallation occurred in both specimens at 1000°C, which was probably associated with the formation of Ti_2AlN between the thick scale and the substrate except for the TiO_2 and α-Al_2O_3.

ACKNOWLEDGEMENTS

This work was financially supported by The Program for Professor of Special Appointment (Eastern Scholar) at Shanghai Institutions of Higher Learning, China, and partly supported by Innovation Program of Shanghai Municipal Education Commission.

REFERENCES

[1] Fleischer RL, Dimiduk DM, Lipsitt HA. Intermetallic Compounds for strong high-temperature materials: status and potential. Ann Rev Mater Sci 1989: 19: 231-63.

[2] Kim YW, Froes FH. High temperature aluminides and intermetallics, TMS, Warrendale, PA, 1989; pp. 2430.

[3] Hayes RW. The creep behavior of the Ti_3Al alloy Ti-24Al-11Nb. Scr Metal Mater 1989; 23: 1931-6.

[4] Rosenstein AH. Overview of research on aerospace metallic structural materials. Mater Sci Eng A 1991; 143: 31-41.

[5] Sagar PK, Banerjee D, Prasad YVRK. Processing of an α-2 aluminide alloy, Ti-24Al-11Nb. Mater Sci Eng A 1994; 177: 185-97.

[6] Mungole MN, Balasubramaniam R, Ghosh A. Oxidation behavior of titanium aluminides of high niobium content. Intermetallics 2000; 8: 717-20.

[7] Wu JS, Zhang LT, Wang F, Jiang K, Qiu GH. The individual effects of niobium and silicon on the oxidation behaviour of Ti_3Al based alloys. Intermetallics 2000; 8: 19-28.

[8] Beye R, Verwerft M, De Hosson JTM, Gronsky R. Oxidation subscale of γ-titanium aluminide. Acta Mater 1996; 44: 4225-31.

[9] Li ZW, Gao W, He YD. Protection of a Ti_3Al-Nb alloy by electro-spark deposition coating. Scr Mater 2001; 45: 1099-1105.

[10] Lee J, Gao W, Li ZW and He YD. Corrosion behaviour of Ti_3Al and Ti_3Al-11 at.% Nb intermetallics. Mater Lett 2003; 57: 1528-38.

[11] Chu MS and Wu SK. Improvement in the oxidation resistance of α_2-Ti_3Al by sputtering Al film and subsequent interdiffusion treatment. Surf Coat Technol 2004; 179: 257-264.

[12] Qian YH, Li MS, Lu B. Isothermal oxidation behavior of Ti_3Al-based alloy at 700-1000℃ in air. Trans Nonferrous Met Soc China 2009; 19: 525-9.

[13] Wu Y, Zhen L and Yang DZ. TEM observation of the α_2/O interface in a Ti_3Al-Nb alloy. Mater Lett 1997; 32: 319-23.

[14] Wu Y, Yang DZ, Song GM. The formation mechanism of the O phase in a Ti_3Al-Nb alloy. Intermetallics 2000; 8: 629-32.
[15] Wu Y, Hwang SK. The effect of aging on microstructure of the O-phase in Ti-24Al-14Nb-3V-0.5Mo alloy. Mater Lett 2001; 49: 131-6.
[16] Wu Y, Zhen L, Yang DZ, Kim MS, Hwang SK, Umakoshi Y. In situ tensile deformation and fracture behavior of Ti-24Al-14Nb-3V-0.5Mo alloy with various microstructures. Intermetallics 2004; 12: 43-53.
[17] Tomasi A, Gialanella S. Oxidation phenomena in a Ti_3Al base-alloy. Thermochim Acta 1995; 269/270: 133-43.
[18] Wallace TA, Clark RK, Wiedemann KE, Sankaran SN. Oxidation characteristics of Ti-25Al-10Nb-3V-1Mo. Oxid Met 1992; 37: 111-24.
[19] Lang C, Schütze M. TEM investigations of the early stages of TiAl oxidation. Oxid Met 1996; 46: 255-85.
[20] Wu Y, Zhen L, Li XW, Yang DZ, Umakoshi Y. Mechanical properties and oxidation behavior of the Ti-24Al-14Nb-3V-0.5Mo alloy sheet. Sci Eng A 2006; 427: 42-50.
[21] Taniguchi S, Shibata T. Influence of additional elements on the oxidation behaviour of TiAl. Intermetallics 1996; 4: S85-S93.
[22] Welsch G, Kahveci AI. In: Grobstein T, Doychack J, Eds. Oxidation of High Temperature Intermetallics Proceeding. Workshop, TMS, Warrendale, USA, 1988; pp. 207-18.
[23] Gil A, Wallura E, Grübmerer H, Quadakkers WJ. The influence of cooling rate during alloy casting on the oxidation behavior of TiAl-based intermetallics. J Mater Sci 1993; 28: 5869-74.

Received: September 24, 2009 Revised: November 1, 2009 Accepted: November 4, 2009